Current Neutralization of Intense MeV Proton Beams Transported in Low-Pressure Gas

F. C. Young,[1] D. D. Hinshelwood,[2] R. F. Hubbard,[1] M. Lampe,[1] J. M. Neri,[1] C. L. Olson,[3] P. F. Ottinger,[1] D. V. Rose,[2] S. P. Slinker,[1] S. J. Stephanakis,[1] and D. R. Welch[4]

[1]*Plasma Physics Division, Naval Research Laboratory, Washington, D.C. 20375*

[2]*JAYCOR, Incorporated, Vienna, Virginia 22182*

[3]*Sandia National Laboratories, Albuquerque, New Mexico 87185*

[4]*Mission Research Corporation, Albuquerque, New Mexico 87106*

(Received 4 February 1993)

This paper reports on the first experiments designed to study ion-beam-induced gas ionization and subsequent conductivity growth using intense proton beams transported through various gases in the 1-Torr pressure regime. Net-current fractions of 2% to 8% are measured outside the beam channel. Ionization is confined predominantly to the beam channel with ionization fractions of a few percent. Analysis suggests that net currents are larger inside the beam channel and that fast electrons and their secondaries carry a significant fraction of the return current in a halo outside the beam.

PACS numbers: 52.40.Mj, 41.85.Ja, 52.25.Jm, 52.65.+z

In ion-driven inertial confinement fusion (ICF), it is necessary to transport intense ion beams over several meters to isolate the ion source from the target explosion and to allow for focusing and time-of-flight bunching. Several light-ion ICF schemes [1], as well as some heavy-ion ICF schemes [2,3], envision ballistic (i.e., field-free) transport and focusing of the beam in neutral gas. This is possible if rapid beam-induced gas ionization leads to formation of a plasma with conductivity sufficient to charge and current neutralize the beam during the pulse duration [4]. Complete charge neutrality is expected; however, large net currents could arise which would shift, and possibly degrade, the beam focal spot [5,6]. The conductivity must also be sufficient to avoid beam filamentation instabilities [7,8] which could disrupt the beam tail. The required conductivity growth results from ion impact ionization, secondary electron impact ionization, electron avalanche breakdown, and late-time Ohmic heating.

The primary light-ion scheme for the proposed Laboratory Microfusion Facility uses ballistic transport with solenoidal lens focusing of 1-MA, 30-MeV, 40-ns lithium beams [9]. A typical beam current density before focusing is of order 1 kA/cm^2. Helium at 1-Torr pressure is suggested for the background gas to satisfy the above requirements while minimizing collisional energy loss and scattering of the beam. Transport in this 1-Torr regime is not well understood. This paper reports on the first experiments designed to study ion-beam-induced gas ionization and subsequent plasma conductivity growth in this regime.

This pressure range falls between the high-density regime treated by resistive models, and the low-density regime treated by collisionless models. To understand this intermediate regime, additional physics must be considered. Fast electrons created by beam-ion impact ionization (i.e., knockon electrons [10] or delta rays), which act to neutralize beam current for ion beams, could be important for intense beams. Also, runaway electrons can result from high electric fields at the beam front. Fast electrons created by these processes can have mean free paths on the order of the beam radius, leading to nonlocal secondary ionization. A significant nonthermal electron population, which persists for the beam pulse duration, can also alter the plasma conductivity. Thus, collisional processes involving both thermal and fast electrons are important in this intermediate regime, and resistive models, which do not treat fast electron effects, are inadequate. Results of theoretical modeling of these experiments using the DYNAPROP [11] and IPROP [12] codes are presented to evaluate the importance of these effects. These codes are described when the modeling results are presented.

The experimental arrangement is shown in Fig. 1. A 1-MeV proton beam, generated in vacuum with a pinch-reflex diode [13] on the Gamble II generator is injected through a 2-μm-thick polycarbonate foil into a collimator consisting of two 3-cm-diam apertures separated by 40 cm. The collimator region is maintained at 1-Torr air to provide reproducible injection into the transport region. A 1-kA/cm^2 beam exits the collimator through another 2-μm-thick polycarbonate foil, and the interaction of this

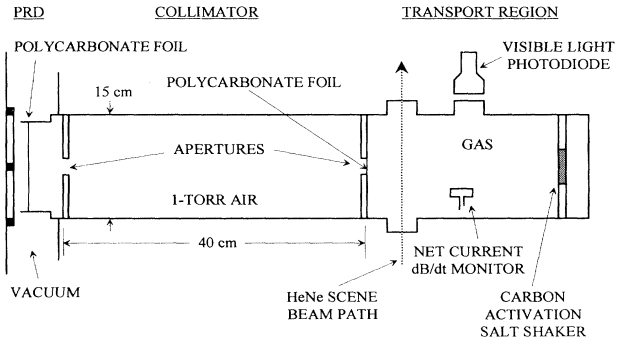

FIG. 1. Experimental arrangement of the pinch-reflex diode (PRD), the collimator, and the transport region.

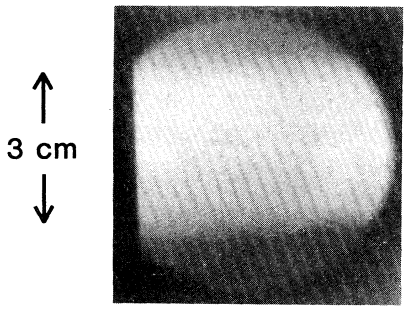

FIG. 2. Visible-light image of the ion-beam excitation of helium at 5 cm into the transport region. The beam is incident from the left.

beam with different gases in the transport region is studied.

The beam itself is characterized using several diagnostics at various distances from the collimator exit. The number of protons in the beam is measured by carbon activation [14]. A "salt shaker" detector located 26 cm beyond the collimator exit is used to minimize blowoff loss of radioactivity [15]. The beam size and uniformity in the transport region are determined from ion-induced $K\alpha$ x-ray images of aluminum targets, and from damage patterns on plastic witness plates. The beam profile is also recorded after transport over 170 cm in gas using chlorostyrene radiachromic film shielded by a 6.4-μm thickness of aluminum. These measurements indicate a uniform beam of 50-mrad divergence with a penumbra extending to 75 mrad, consistent with the collimator geometry. The energy distribution of ions in the beam is measured using a stacked-foil diagnostic as described below.

Interaction of the beam with the gas is diagnosed using photometry, magnetic-field measurements, and interferometry. Visible light emitted from the gas is monitored with a photodiode and a framing camera. A visible-light image, recorded 5 cm beyond the collimator exit with a 400-ns gated camera, is shown in Fig. 2. This image is uniform with no apparent structure. Net currents are recorded with a dB/dt monitor located 13 cm downstream of the collimator exit and outside the beam envelope at 4 cm radius. A HeNe interferometer using heterodyne phase detection is used to determine the electron density [16]. This technique provides high sensitivity and signal-to-noise ratio at the expense of time resolution. The sensitivity for this setup is limited by the noise-equivalent-average density of 5×10^{14} cm^{-3}, with a time resolution of 25 ns. The path of the interferometer scene beam is 5 cm from the collimator exit as shown in Fig. 1.

Data from a typical shot are shown in Fig. 3. Current and voltage traces in the diode [Fig. 3(a)] indicate that a 50-ns-duration, >400-kA ion pulse is generated with most of the ions in the range of 1.0 to 1.2 MV. Adjusting

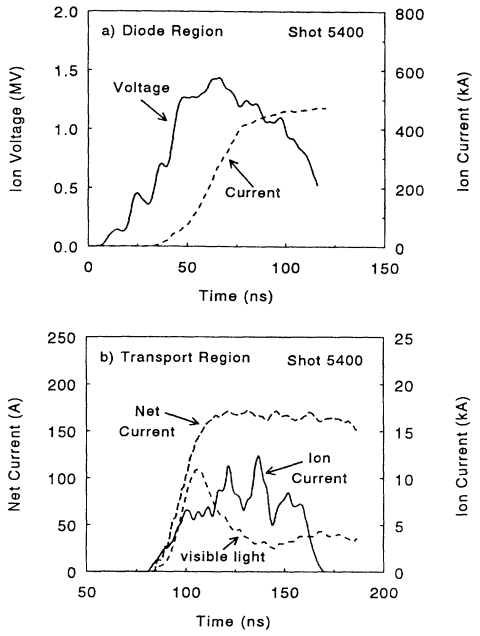

FIG. 3. (a) Ion-voltage and ion-current traces in the diode and (b) time-of-flight shifted ion current compared with measured net-current and visible-light traces.

this pulse for proton time of flight results in the ion-current pulse in Fig. 3(b) in the transport region. This pulse includes only protons above the 460-keV thick-target carbon-activation threshold and is normalized to the number of protons determined from this activation. This pulse duration is evaluated for each shot to determine the average proton current in the transport region. The net-current trace and the visible-light emission begin when the ion beam reaches the transport region.

The energy spectrum of the proton beam is measured in 1-Torr air with a carbon-activation foil stack located at 170 cm from the collimator exit. At this distance, a stack of ten 2-μm-thick polycarbonate foils with a 1.8-μm-thick aluminum cover survives, and the ^{13}N activity in each foil can be measured after the shot. A foil area of 124 cm^2 is used to provide measurable activity. The activity in each foil, produced by the 37-keV FWHM $^{12}C(p,\gamma)^{13}N$ resonance at 460 keV, is unfolded using the range-energy relation for protons in polycarbonate ($C_{16}H_{14}O_3$) to give the solid histogram in Fig. 4. The width of each step in this histogram corresponds to the energy interval over which protons activate that foil in the stack. This spectrum has been shifted up in energy to correct for energy loss in the aluminum cover on the stack. The dashed histogram is the spectrum determined from the diode current and voltage for this shot. It has been shifted down in energy to correct for energy loss in the two polycarbonate foils and air in the collimator and transport regions. Note the 400× difference in these two scales. The spectral intensity in the transport region is

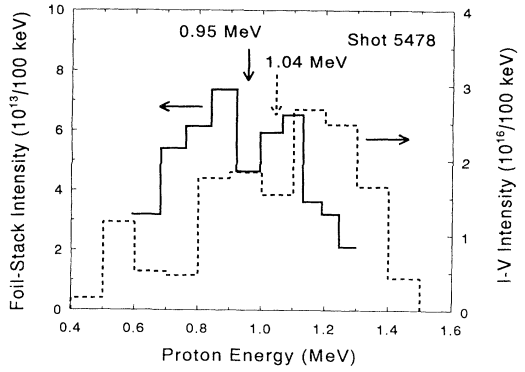

FIG. 4. Histograms of proton number vs proton energy in the transport region deduced from stacked-foil activations (solid) and from the diode current and voltage (dashed). Average energies for these histograms are indicated.

TABLE I. Net current and electron density measurements.

Gas	Pressure (Torr)	Proton current (kA)	Peak net current (kA)	Electron density (10^{15} cm^{-3})
Ne	0.34	4.5	0.11	...
	1.0	6.3	0.20	1.6
	1.25	6.4	0.22	...
	4.0	4.6	0.17	2.6
Air	0.25	4.8	0.18	...
	1.0	6.9	0.21	0.9
	4.0	5.5	0.28	1.8
He	0.25	6.2	0.31	...
	1.0	6.8	0.32	0.7
	4.0	5.9	0.47	1.5

only a small fraction of that in the diode and corresponds to somewhat lower-energy protons. Average energies for these two spectra differ by about 100 keV. Since most of the protons have energies less than 1 MeV and the deuteron fraction in the beam is unknown, no correction is made for carbon activation by deuterons [14].

Simulations using a ray-trace code and a diode model [17] for the pinch-reflex diode have been carried out to calculate beam transport through the collimator and into the transport section. Experimental diode voltage and current wave forms and a beam microdivergence of 125 mrad at the anode were used to generate the time-dependent ion distribution function. Complete charge and current neutralization of the beam are assumed and ion energies are corrected for losses in the foils and gas. Ions which hit aperture plates or walls are removed from the simulation. Results predict beam currents, radial density profiles, and divergences which agree with those observed in the transport region. The predicted energy spectrum, however, agrees with the dashed curve in Fig. 4 rather than the measured spectrum (solid curve). An electric field induced at the beam front by a rising net current could explain the lower energy of the measured spectrum. Higher-energy ions, which reside at the beam head, would be slowed by this induced field. Because complete current neutralization is assumed, this energy loss is precluded in the simulations. If this is the correct explanation for the observed energy spectrum, the downshift would be considerably less at the collimator exit than at 170 cm downstream where the measurement was made.

Net currents and electron densities were measured for helium, neon, and air at pressures ranging from 0.25 to 4 Torr. Peak values of these measurements are given in Table I. From shot to shot the average current of the incident proton beam ranged from about 5 to 7 kA corresponding to current densities of about 0.7 to 1 kA/cm^2 at the collimator exit. Net current wave forms from the dB/dt monitor have current rise times of 15 to 50 ns and decay times of several hundred ns. The uncertainty in the peak net currents is estimated to be +10%. Net-current fractions range from 2.3% to 8.0%. The local electron density is obtained by dividing the interferometrically measured line density by the 3-cm beam diameter. Peak electron densities are of order 10^{15} cm^{-3} and correspond to ionization fractions of 0.6% to 4.6%. For 0.25-Torr gas pressure, electron densities are too small to be measured. Negligible line density (less than the instrument sensitivity) was observed when the scene beam was located about 1.5 cm off center, indicating that ionization is largely confined to the beam diameter.

DYNAPROP and IPROP simulations were carried out to evaluate beam-induced net currents and electron densities in helium. DYNAPROP is a 1D code which uses a resistive model to treat plasmas created by beam interaction with high-density collisional gases. Beam dynamics is described by envelope and emittance equations; the plasma density, temperature, and conductivity are determined by rate equations; and the net current is calculated with a circuit equation. IPROP is a 3D hybrid code which treats beam ions and fast electrons (above 100 eV) as particles. The remaining electrons are treated as a resistive medium, while plasma ions are represented as a stationary background. Rate equations are used to create electron-ion pairs and Maxwell's equations are used to solve for the fields. Because azimuthal symmetry is assumed, IPROP was used in $2\frac{1}{2}$ D mode.

Results are compared with the measurements in Table II. For all three pressures, IPROP predicts a net current inside the dB/dt probe ($r=4$ cm) that is within 30% of the measured value. However, IPROP predicts a net current within the 1.5-cm beam radius that is a factor of 3 larger than the measured values. DYNAPROP calculates the effective net current (a radially averaged current weighted by the beam current density), which is predicted to be somewhat larger than the IPROP current within

TABLE II. Comparisons with theory for helium.

Pressure (Torr)	Net currents (kA) Measured ($r=4$ cm)	IPROP ($r=4$ cm)	IPROP ($r=1.5$ cm)	DYNAPROP ($r\approx 1.5$ cm)	Electron densities (10^{15} cm^{-3}) Measured (line average)	IPROP ($r=0$)	IPROP ($r=1.5$ cm)	DYNAPROP ($r=0$)
0.25	0.31	0.31	0.9	1.3	...	0.2	0.2	0.2
1.0	0.32	0.39	1.0	1.5	0.7	1.0	0.6	0.7
4.0	0.47	0.63	1.6	2.1	1.5	3.2	1.8	1.9

the beam radius. The small net current at the probe location observed in IPROP is a consequence of fast electrons carrying a significant fraction of the return current in a halo outside the beam. These electrons create additional ionization at large radius which contributes to the return current. These comparisons suggest that fast electrons play an important role in return-current conduction, and that the magnetic field within the beam channel is larger than that measured outside the beam envelope. An effective net-current fraction of about 25% in the ray-trace calculations mentioned earlier would be required to down-shift the high energy edge of the calculated spectrum to match the solid histogram in Fig. 4. This fraction is consistent with IPROP and DYNAPROP predictions within the beam. Both IPROP and DYNAPROP predict electron densities that are in reasonable agreement with the measured values.

In summary, 1-MeV, 1-kA/cm^2 proton beams have been transported through helium, neon, and air at pressures of 0.25 to 4 Torr. Small net current fractions of 2% to 8%, are measured outside the beam channel. Ionization is confined predominantly to the beam channel where ionization fractions are only a few percent. Analysis of the beam energy spectrum after transport suggests that larger effective net currents exist inside the beam channel. Similarly, IPROP and DYNAPROP calculations predict net currents in the beam channel 3 to 5 times larger than measured net currents. Outside the beam channel, IPROP predicts small net currents in agreement with measurements. Fast electrons and their secondaries carry a significant fraction of the return current outside the beam (although their density is low compared with the plasma electron density within the beam channel). More extensive experiments and modeling are required to develop sufficient understanding of beam-induced gas ionization and conductivity growth in this pressure regime to confidently scale results to ICF scenarios.

The expert assistance of J. R. Boller and B. Roberts in supporting these experiments is appreciated. This work was supported by the U.S. Department of Energy through Sandia National Laboratories.

[1] D. Mosher *et al.*, in *Proceedings of the Eighth International Conference on High-Power Particle Beams*, edited by B. N. Breizman and B. A. Knyazev (World Scientific, Singapore, 1991), p. 26.
[2] C. L. Olson, J. Fusion Energy **1**, 309 (1982).
[3] *Proceedings of the Conference on Heavy Ion Inertial Fusion, Washington, DC, 1986*, AIP Conf. Proc. No. 152 (American Institute of Physics, New York, 1986).
[4] C. L. Olson, in *Proceedings of the 1990 Linear Accelerator Conference, Albuquerque, New Mexico, September 1990* (LANL Report No. LA-12004-C), p. 396.
[5] J. A. Swegle and S. A. Slutz, J. Appl. Phys. **60**, 3444 (1986).
[6] D. J. Johnson *et al.*, J. Appl. Phys. **58**, 12 (1985).
[7] C. L. Olson, in *Proceedings of the 1991 IEEE Conference on Plasma Science, Williamsburg, Virginia, June 1991, IEEE Conference Records–Abstracts*, edited by K. Schoenbach (IEEE, New York, 1992), p. 165.
[8] E. P. Lee *et al.*, Phys. Fluids **23**, 2095 (1980).
[9] P. F. Ottinger, D. V. Rose, J. M. Neri, and C. L. Olson, J. Appl. Phys. **72**, 395 (1992).
[10] R. F. Hubbard, S. A. Goldstein, and D. Tidman, in *Proceedings of the Heavy Ion Beam Fusion Workshop, Berkeley, California, 1979*, edited by W. B. Hermannsfeldt (Lawrence Berkeley Laboratory Report No. LBL-10301, 1980), p. 488.
[11] See R. F. Hubbard *et al.*, NRL Memorandum Report No. 7112, 1992 (National Technical Information Service Document No. ADA256070). Copies may be ordered from the National Technical Information Service, Springfield, VA 22161. The price is $17.50 plus a $3.00 handling fee. All orders must be prepaid.
[12] B. B. Godfrey and D. R. Welch, in *Proceedings of the Twelfth Conference on Numerical Simulations of Plasmas* (Lawrence Livermore National Laboratory, San Francisco, CA, 1987), Paper CM1.
[13] S. J. Stephanakis *et al.*, Phys. Rev. Lett. **37**, 1543 (1976).
[14] F. C. Young, J. Golden, and C. A. Kapetanakos, Rev. Sci. Instrum. **48**, 432 (1977).
[15] A. E. Blaugrund and S. J. Stephanakis, Rev. Sci. Instrum. **49**, 866 (1978).
[16] B. V. Weber and D. D. Hinshelwood, Rev. Sci. Instrum. **63**, 5199 (1992).
[17] J. M. Neri *et al.*, Phys. Fluids B **5**, 176 (1993).

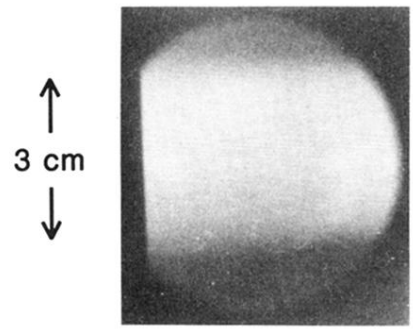

FIG. 2. Visible-light image of the ion-beam excitation of helium at 5 cm into the transport region. The beam is incident from the left.